

June 2022

The Thermodynamics of a Stochastic Geometry Model with Applications to Non-Extensive Statistics

O.K. Kazemi

University of Mazandaran, Babolsar, Iran, o.kazemi@stu.umz.ac.ir

A. Pourdarvish

University of Mazandaran, Babolsar, Iran, a.pourdarvish@umz.ac.ir

J. Sadeghi

University of Mazandaran, Babolsar, Iran, pouriya@ipm.ir

Follow this and additional works at: <https://digitalcommons.lsu.edu/josa>



Part of the [Analysis Commons](#), and the [Other Mathematics Commons](#)

Recommended Citation

Kazemi, O.K.; Pourdarvish, A.; and Sadeghi, J. (2022) "The Thermodynamics of a Stochastic Geometry Model with Applications to Non-Extensive Statistics," *Journal of Stochastic Analysis*: Vol. 3: No. 2, Article 5.

DOI: 10.31390/josa.3.2.05

Available at: <https://digitalcommons.lsu.edu/josa/vol3/iss2/5>

THE THERMODYNAMICS OF A STOCHASTIC GEOMETRY MODEL WITH APPLICATIONS TO NON-EXTENSIVE STATISTICS

O. K. KAZEMI*, A. POURDARVISH, AND J. SADEGHI

ABSTRACT. We use the escort distribution instead of the original distribution for calculating the moment generating function and the physical quantities in non-extensive statistical mechanics. According to the associated escort distribution, we obtain the moment generating function for some random variables. In the following, we consider the model of continuum percolation in stochastic geometry and percolation theory which is obtained by connecting the Poisson points with a probability that depends on their relative position. Using a formal expression for the probability of the size of a cluster at the origin provided by Penrose, we derive the q -thermodynamic quantities to evaluate these quantities performance in obtaining the critical point when the percolation occurs. Also, by plotting the q -thermodynamic quantities, we show very interesting fluctuations at the critical point.

1. Introduction

The discussion of mathematical and stochastic models of infectious diseases, which are widely used in epidemiology, is of interest to every human community. These models provide an understanding of the underlying mechanisms by which epidemic outbreaks in a given population are addressed. In this way, decisions can be made to control or prevent the epidemic [27]. One of the most widely used mathematical models to describe this type of problem is a random connection model (RCM), also known as a soft random geometric graph [22]. The RCM of continuum percolation is a generalization of random geometric graph with two sources of randomness, the point locations and their links. In this model, the probability of existence of an edge between two points decreases as the distance between the two points increases [23].

The RCM is quite general and has applications in different branches of science [11, 5, 8]. In physics, continuum percolation is applied to study clustering behavior of particles in continuum systems and is relevant to phenomena like conduction in dispersions, flow in porous media, elastic behavior of composites, solgel transition in polymers, aggregation in colloids, and the structure of liquid water [22]. The special case of the RCM is obtained when the connection function is

Received 2021-9-10; Accepted 2022-6-26; Communicated by the editors.

2020 *Mathematics Subject Classification.* 60D05; 60K35; 82B30; 05C80.

Key words and phrases. Thermodynamics, non-extensive statistical mechanics, stochastic geometry, Poisson point process, moment generating function.

* Corresponding author.

of the Boolean, zero-one type. Such a model is the simplest Boolean model of continuum percolation in stochastic geometry and percolation theory [14]. This is the most basic random geometric graph and a central object in random graph theory, which is the so-called Gilbert graph or Poisson blob model [24]. Although Gilbert's main focus was the study of communications networks, he noted that a resulting infinite graph could also model the spread of a contagious disease [7]. Gilbert discussed percolation theory by defining a critical parameter when an infinitely connected cluster is formed. In other words, for parameters larger than the critical parameter, there is a non-zero probability that the disease spreads, or that communication is possible to some arbitrarily distant nodes of the network. In this case, we say that the model percolates. According to a connectivity and percolation theory are the most important focus of much research [8], this paper studies such certain properties by the use of statistical mechanics tools.

Statistical mechanics provides an interpretation of the molecular level of macroscopic thermodynamic quantities such as labor, heat, free energy, and entropy. For more than a century, the Boltzmann-Gibbs statistical mechanic has played an important role in discovering the thermodynamics of systems from mechanical details in the equilibrium conditions. These types of systems are simple and clearly show that their free energy and entropy are extensive, which means that if two identical systems combine, the entropy and free energy of combined system are equal to summation of entropy and free energy of its subsystems [21]. Over the past century, physicists have noticed that there are many statistical systems in nature that cannot be described by the Boltzmann-Gibbs statistical mechanics. This theory is ineffective in interpreting small systems or with complex interactions and long-term correlations [3]. Because such systems are often non-extensive, we need a non-extensive statistical mechanics capable of interpreting such systems [28]. The ideas related with non-extensive statistical mechanics have received an enormous amount of applications in a variety of disciplines. It enables to analyzing systems such as class of physical ensembles involving long-range interactions, long-time memories, or (multi-)fractal structures [2, 29]. There is a controversy in the area of non-extensive statistical mechanics regarding the form of the expectation value of a physical quantity. Two definitions have been discussed for expectation value of a physical quantity: one is the ordinary definition and the other is the normalized q -expectation value associated with the escort distribution [4].

Using the Shore-Johnson theorem and the idea of the normalized q -expectation value, we examine the idea of the q -statistical moments. That is, given that many thermodynamic quantities in statistical mechanics are a function of the distribution of the system on microscopic states, we substitute the escort distribution for the system distribution. So, we describe the q -moment generating function formalism and discuss the main ideas. We consider some statistically important discrete and continuous random variables and calculate the escort distribution and the moment generating function of these variables. Finally, we discuss the concept of phase transition and percolation by examining some q -thermodynamic quantities [15] and the q -moments of the probability distribution, including free energy, entropy, zero-field free energy, mean, variance and kurtosis [17, 20]. As we know, the fluctuations play a central role in our understanding of phase transitions. The

interesting thing we have observed is that the fluctuations of all studied quantities for the RCM with the connection function $g(x) = I_{\{|x| \leq 1\}}$ and using the escort distribution, clearly reveal the critical point.

These purposes give us a motivation to organize this paper as follows. In the section 2, we describe the RCM and define the thermodynamic quantities used throughout this paper. The results are discussed in the section 3. In the subsection 3.1, using the escort distribution, the moment generating function are calculated and expressed in detail. Finally, in the subsection 3.2, the q -thermodynamic quantities are obtained and plotted to determine the phase transition in this model.

2. The Introduction to a Continuum Percolation Model

We consider the RCM of continuum percolation where the points x and y of a homogeneous Poisson point process are connected with probability $g(|x - y|)$ for a given g . $|\cdot|$ denotes the Euclidean norm (Gilbert's graph is the special case of the RCM with $g(x) = I_{\{|x| \leq r\}}$ [12]). The RCM in Euclidean space \mathbb{R}^d with connection function g can be described as follows: let $\eta' = \{x_1, x_2, \dots\}$ be a homogeneous Poisson point process with intensity ρ on \mathbb{R}^d and $g : \mathbb{R}^d \rightarrow [0, 1]$ be a measurable and symmetric function and that $0 < \int_{\mathbb{R}^d} g(x) dx < \infty$. Fix $x_0 = 0$, the origin, and let $\eta = \{x_0, x_1, \dots\}$. Given two points x_i and x_j of η (with $i > j$), connect them by an edge with probability $g(|x_i - x_j|)$ independently of all other pairs of points and the process η . This yields the RCM, an undirected random graph $G(\eta)$ with vertex set η . A component (cluster) of this graph is a maximally connected subset of η . The cluster at the origin, $C(0)$, is the vertex set of the connected component of G which contains the origin [14]. Denote by $n[C(0)]$ the number of points (including 0) in $C(0)$, so that $n[C(0)]$ is a random variable taking values in $\{1, 2, \dots\}$.

Let $p_k(\rho)$ denote the probability, when η has intensity ρ , that $C(0)$ consists of k points. That is,

$$p_k(\rho) = p(n[C(0)] = k), \quad k = 1, 2, \dots$$

Theorem 2.1. *For any measurable and bounded set Υ on \mathbb{R}^d and $k \in \{1, 2, \dots\}$ [24] proved, in any dimension, that*

$$\begin{aligned} p_k(\rho) &= p_\rho(n[C(0)] = k, C(0) \subset \Upsilon) \\ &= \rho^{(k-1)} / (k-1)! \int_{\Upsilon} \cdots \int_{\Upsilon} g_2(0, x_1, \dots, x_{k-1}) \\ &\quad \times \exp\{-\rho \int_{\Upsilon} g_1(y; \{0, x_1, \dots, x_{k-1}\}) dy\} dx_1 \dots dx_{k-1} \end{aligned} \quad (2.1)$$

In this theorem, g_1 denote the probability that x_0 is not isolated in this random graph [22]. That is

$$g_1(x_0; x_1, \dots, x_k) = 1 - \prod_{j=1}^k (1 - g(x_0 - x_j)) \quad (2.2)$$

and, $g_2(x_0, x_1, \dots, x_k)$, the probability that the random graph G is connected, is [9]

$$g_2(x_0, x_1, \dots, x_k) = \sum_{G \in G_{k+1}^c} \prod_{(i,j) \in G} g_{ij} \prod_{(i,j) \in G} (1 - g_{ij}),$$

where the summation is over all connected graphs G_{k+1}^c on points of c and largest cluster of size $(k+1)$ ($c = \{x_0, \dots, x_k\}$).

Penrose [24] rigorously derived this integral for $p_k(\rho)$ in any dimension d , which this probability can be computed rather handily in one dimension. But, this integral cannot be calculated analytically and hence requires an approximate evaluation in the higher dimension. Penrose [25] provided an approximation of this probability function in a particular case. He considered the homogeneous Poisson process of rate $\rho = y/c_d$ on \mathbb{R}^d for $y > 0$, where $c_d = \pi^{(d/2)}/\Gamma((d/2) + 1)$ is the volume of the ball of unit radius in dimension d . In this paper, it is proved that for the connection function $g(x) = pI_{\{|x| \leq r\}}$ ($r = 1, p = 1$) as $d \rightarrow \infty$ with constant y , the following limit relation is established.

$$p_k(\rho) \rightarrow p_k(y) = \frac{k^{k-2}}{(k-1)!} y^{k-1} e^{-ky}, \quad k = 1, 2, 3, \dots \quad (2.3)$$

As mentioned, $p_k(\rho)$ is the cluster distribution. By analogy with the Ising model, we introduce the magnetization function as [31]

$$M(\rho, h) = 1 - \sum_{k=0}^{\infty} p_k(\rho) e^{-kh}, \quad h \geq 0, \quad (2.4)$$

where h is the external magnetic field. By setting $h = 0$ in the magnetization function,

$$M(\rho, 0) = p(n[C(0)] = \infty).$$

Using the term by term differentiation, we have

$$\lim_{h \rightarrow 0^+} \frac{\partial M(\rho, h)}{\partial h} = \mathbb{E}_\rho[n[C(0)]I_{\{n[C(0)] < \infty\}}] = \chi^{(1)}(\rho).$$

$\chi^{(1)}(\rho)$ which is obtained by differentiating the magnetic field M with respect to h , is called the mean cluster size. It is the analogue of the (isothermal) susceptibility of magnetic systems. Also, for any $N \in \mathbb{R}$, the following limit relationship is established.

$$(-1)^{(N+1)} \lim_{h \rightarrow 0^+} \frac{\partial^N M(\rho, h)}{\partial h^N} = \mathbb{E}_\rho[n[C(0)]^N I_{\{n[C(0)] < \infty\}}] = \chi^{(N)}(\rho). \quad (2.5)$$

More precisely, $\chi^{(N)}(\rho)$ is the N^{th} moment of the size of the cluster at an arbitrary point of Γ , discounting infinite clusters. The free energy $F(\rho, h)$ is defined by [32]

$$F(\rho, h) = h(1 - p_0(\rho)) + \sum_{k=1}^{\infty} \frac{1}{k} p_k(\rho) e^{-kh}, \quad h \geq 0. \quad (2.6)$$

The second term in the above equation was first presented by Kasteleyn and Fortuin to regulate a correspondence between values for percolation and similar

values for magnetic systems. If we differentiate the free energy $F(\rho, h)$ with respect to h , we get

$$\frac{\partial F(\rho, h)}{\partial h} = M(\rho, h).$$

The zero-field free energy $F(\rho, 0)$ is a more interesting subject of study [16]. By our definition,

$$\begin{aligned} F(\rho, 0) = \mathbb{E}_\rho[n[C(0)]^{-1}I_{\{n[C(0)] < \infty\}}] &= \sum_{k=1}^{\infty} \frac{1}{k} p_k(\rho) \\ &= \chi^{(-1)}(\rho). \end{aligned} \quad (2.7)$$

Grimmett [13] discovered that the zero-field free energy or the cluster density coincides with the number of clusters per vertex. Penrose in [24] proved the continuity of the cluster density in ρ for the case $g(x) = I_{\{|x| \leq r\}}$. Also, he gave upper and lower bounds the zero-field free energy for this connection function.

On the other hand, the Helmholtz free energy [19] is

$$F = U - \beta S, \quad (2.8)$$

The functions of U and S are called the internal energy (the mean cluster size) and the entropy, respectively. Also, β is a fixed number. Here, we consider the BG-shannon entropy as

$$S = - \sum_{k=0}^{\infty} p_k(\rho) \log p_k(\rho). \quad (2.9)$$

3. Main Results

We want to evaluate the performance of the cluster probability function and its thermodynamic quantities when using their non-extensive forms. For this purpose, in the first subsection, we introduce the moment generating function of some special discrete and continuous probability distributions in the non-extensive state. Using the material presented in this subsection, we will refer to one of the applications in physics in the next subsection. We present some of the important physics quantities in the evaluation of the percolation event based on non-extensive statistical mechanics.

3.1. The Moment Generating Function According to The Escort Distribution. The concept of the escort distributions has been introduced by Beck and Schlögl [6] in order to scan the attributes of the original distributions describing the (multi)fractal features of nonlinear dynamical systems. Let p_i be the original distribution. Then, the escort distribution associated with it is given by [1].

$$P_i = \frac{\phi(p_i)}{\sum_{j=1}^{\infty} \phi(p_j)}, \quad \sum_{i=1}^{\infty} P_i = 1 \quad (3.1)$$

where ϕ is a certain positive function. Of particular importance is the case, $\phi(s) = s^q$ ($0 \leq s \leq 1, q > 0$), and correspondingly

$$P_i = \frac{(p_i)^q}{\sum_{j=1}^{\infty} (p_j)^q}. \quad (3.2)$$

The parameter q , is referred to as the order of P_i . The problem concerning the definition of expectation value of a physical quantity seems to be poorly understood. We mention that the (generalized) expectation value with respect to P_i in (3.2), termed the q -expectation value, plays a crucial role in the formulation of non-extensive statistical mechanics [3]. In fact, there are two different definitions in the literature. One is the frequently employed definition, which is the normalized q -expectation value [30]:

$$\mathbb{E}_q(\varepsilon) = \sum_{i=1}^{\infty} P_i \varepsilon_i, \quad (3.3)$$

where ε is a physical random variable under consideration (e.g., the system energy) with its i th value ε_i . The other definition is the ordinary one

$$\mathbb{E}_1(\varepsilon) = \sum_{i=1}^{\infty} p_i \varepsilon_i, \quad (3.4)$$

which is preferred by some researchers [1].

Generally, in the probability theory and statistics, the moment generating function of a real-valued random variable is an alternative specification of its probability distribution. Thus, it provides the basis of an alternative route to analytical results compared with working directly with probability density functions. There are particularly simple results for the moment generating functions of distributions defined by the weighted sums of random variables. However, not all random variables have moment generating functions. As its name implies, the moment generating function can be used to compute a distribution's moments: the N^{th} moment about 0 is the N^{th} derivative of the moment generating function, evaluated at 0. The moment generating function of a random variable X defined as

$$M_X(t) := \mathbb{E}(e^{tX}), \quad t \in \mathbb{R}, \quad (3.5)$$

for which the expectation $\mathbb{E}(\cdot)$ is well defined. Using the escort distribution (3.2), the q -moment generating function values in discrete distributions is computed as

$$M_{X,q}(t) := \sum_{x=1}^{\infty} e^{tx} P_x \quad (3.6)$$

The most important application of the moment generating function method is to find the distribution of the random variable $Y = X_1 + X_2 + \dots + X_n$ in which X_1, X_2, \dots, X_n are independent random variables. We can express this result in the non-extensive discussion this way. If X_1, X_2, \dots, X_n are independent random variables and the moment generating function of each of them exists for

all values of t in the $(-h, h)$ interval, in which h is a positive number, and $Y = X_1 + X_2 + \dots + X_n$, then

$$M_{Y,q}(t) = \mathbb{E}_q[e^{(\sum_{i=1}^n X_i)t}] = \prod_{i=1}^n M_{q,X_i}(t), \quad -h < t < h. \quad (3.7)$$

Here, we obtained the escort distributions, q -expectation and q -moment generating function values for some random variables.

In the first case, suppose $X \in \{0, 1\}$ has the Bernoulli distribution with some parameter $0 \leq p \leq 1$. The escort distribution of this distribution also has the Bernoulli distribution with the probability of success $P_1 = \frac{p^q}{p^q + (1-p)^q}$. The values of the q -expectation and the q -moment generating function for this distribution can be easily calculated, using equations (3.3) and (3.6), respectively.

In the second case, consider the discrete uniform distribution with the probability mass function,

$$p(x) = \frac{1}{k}, \quad x = 1, 2, \dots, k \quad (3.8)$$

In this case, the escort distribution is exactly equal to (3.8). The generating functions of this distribution are given in [18].

For the next example, suppose the random variable X has the geometric distribution with a success parameter p . The escort distribution of this distribution also has the geometric distribution with success parameter $(1 - (1 - p)^q)$.

The next distribution that its non-extensive properties are discussed here is the Poisson distribution with an integer parameter λ . The escort distribution of this probability function is

$$P_x = \frac{(\lambda^x / x!)^q}{\sum_{j=0}^{\infty} (\lambda^j / j!)^q}, \quad x = 0, 1, 2, \dots \quad (3.9)$$

The q -expectation and q -moment generating are calculated using the formulas expressed in (3.3) and (3.6). By plotting changes of the q -expectation and q -variance ($V_q(X) = \mathbb{E}_q(X^2) - \mathbb{E}_q(X)^2$) versus q , we see an interesting trend in these changes. The q -expectation and q -variance of this distribution with different parameters λ are shown in the parts of (a) and (b) of Figure 1. As shown in this Figure, from order q onwards, the q -expectation and q -variance of this escort distribution converge to a number. On the q -expectation, for each value of the parameter λ , the graph starts from the parameter λ and is fixed by decreasing by half, whereas for each parameter of λ , the q -variance graph starts from parameter λ and converges to 0.25.

Finally, we evaluate the escort distribution of a continuous and widely used statistical distribution, the Normal distribution. The escort distribution of the Normal distribution with parameters μ and σ is the Normal distribution with parameters μ and σ/\sqrt{q} . The illustration of this escort distribution with parameter $\mu = 0$ and $\sigma = 2/\sqrt{q}$ for different values of q is shown in Figure 1. According to this Figure, decreasing the value of q leads to an increase in variance, and as a result, the values of the escort distribution P_x approach the surface.

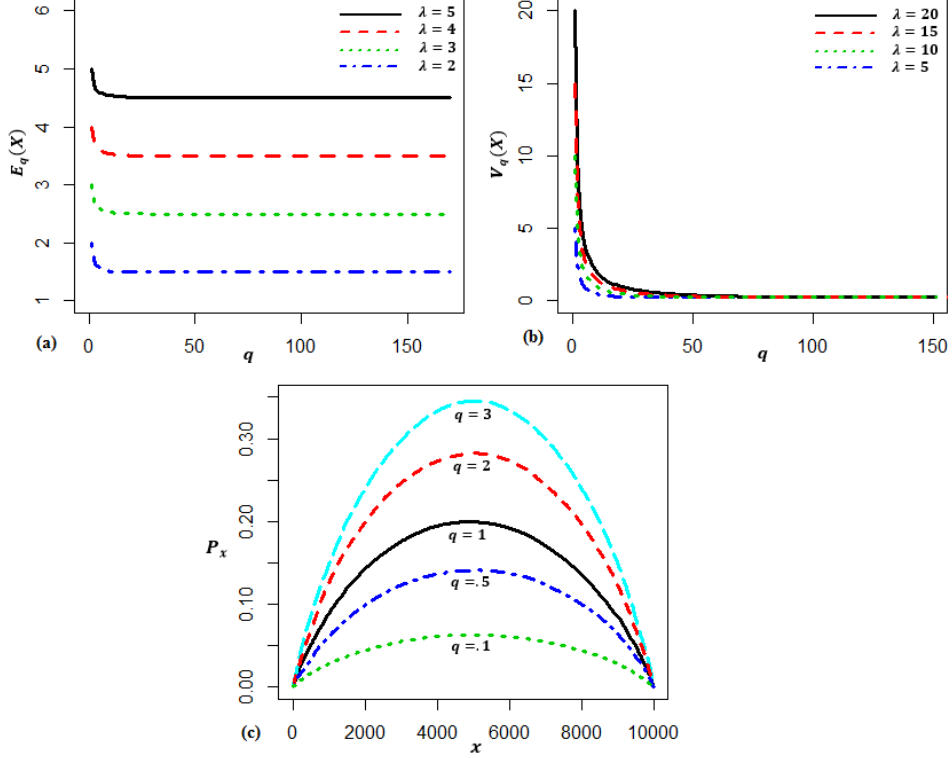


FIGURE 1. The illustration of the q -expectation (a) and the q -variance (b) of the Poisson distribution with the different parameters λ versus the values q and the escort distribution of the Normal distribution with the parameters μ and σ (c).

3.2. The q -Thermodynamics Based on Poisson Point process. Now, we want to discuss a very interesting concept called percolation using the change we made to the probability function. This change involves the use of the escort distribution with different values q . As discussed in the subsection 3.1, we obtained the escort distribution of some random variables and the moment characteristics of these distributions. The escort distribution of the approximation function provided by Penrose (2.3) in the RCM is

$$\begin{aligned}
 P_{q,k}(y) &= \frac{(p_k(y))^q}{\sum_{j=1}^{\infty} (p_j(y))^q} \\
 &= \frac{\left[\frac{k^{k-2}}{(k-1)!} \right]^q y^{q(k-1)} e^{-qky}}{\sum_{j=1}^{\infty} \left[\frac{j^{j-2}}{(j-1)!} \right]^q y^{q(j-1)} e^{-qjy}}, \quad k = 1, 2, 3, \dots \quad (3.10)
 \end{aligned}$$

The variations of this function in terms of cluster size, k , for different values of q and y are shown in the 3D plots of Figure 2.

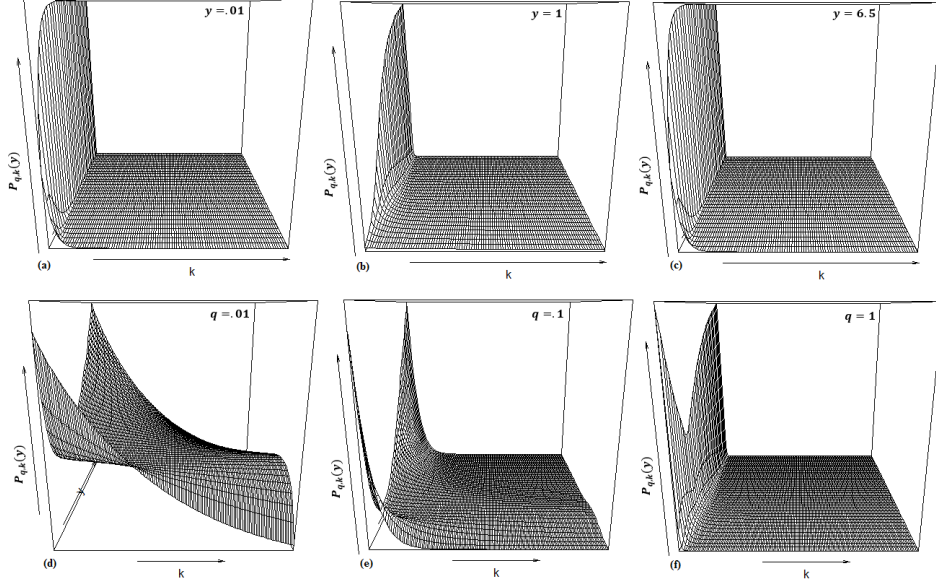


FIGURE 2. The variations of the escort distribution of the approximation function provided by Penrose in the RCM in terms of k , for the different values q and y .

The parts (a), (b) and (c) of this Figure show the escort function (3.10) in terms of $k \in [1, 140]$ and $q \in [0.1, 4]$. A very interesting point that can be clearly seen in these three Figures is the recursive process of the function for $y < 1$ and $y > 1$. Also, the 3D plot of this escort function in terms of $k \in [1, 140]$ and $y \in [0.1, 4]$ for three different values of q is drawn in the parts (d), (e) and (f) of Figure 2. For the small values q , two arcs are seen in the two left corners of the images, which decrease in depth as the value q increases. One thing we see is that the arc changes exactly at the point $y = 1$. Therefore, by drawing these 3D shapes, we clearly see the changes in the escort probability function for $y = 1$ and the values around this point. In fact, this point is called the critical point or critical intensity, that is, where the percolation occurs [10]. In the RCM's, the percolation probability, that is, the probability that there exists an infinite cluster is

$$\psi(\rho) = P(n[C(0)] = \infty),$$

and the critical intensity defined as

$$\rho_c = \sup \{ \rho : \psi(\rho) = 0 \}.$$

Based on the fundamental theorem presented by Penrose, it is shown that $y_c (= \rho_c d) \in (0, \infty)$ and $\lim_{d \rightarrow \infty} y_c = 1$ [25]. Here we want to present mathematical and physical analytical methods for this critical point. In the physics literature,

matter has different states. For instance, gas, liquid, solid, magnetic ordering, superconducting and superfluid states can exist in different materials. When the matter transits from one state to another state, phase transition occurs in the system. In standard statistical physics, the histogram of thermodynamic quantities

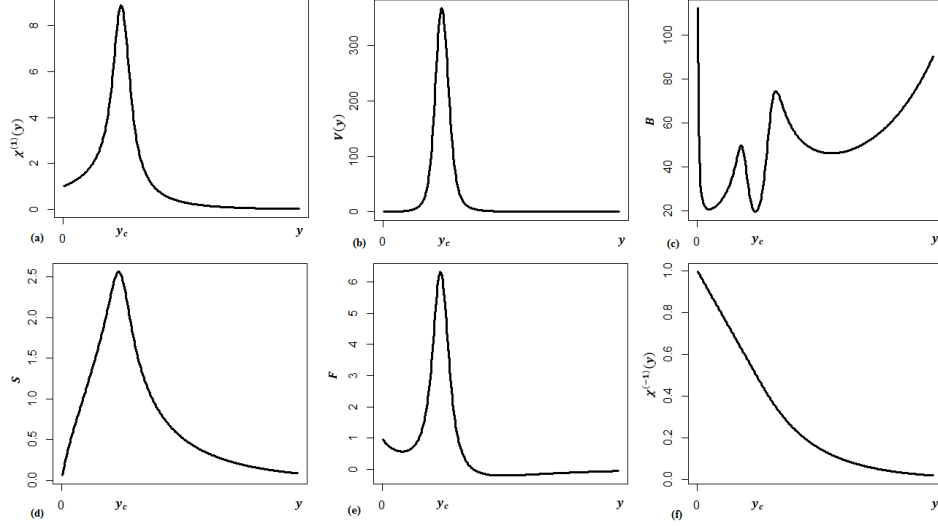


FIGURE 3. The thermodynamic quantities versus the intensity parameter in the RCM.

is often used to detect the nature of a phase transitions and the percolation point. Among these quantities that can be examined are the cluster mean, variance, kurtosis, entropy, free energy and the zero-field free energy for the approximation function provided by Penrose in the RCM. These quantities are shown in Figure 3 versus intensity parameter. From these diagrams, we can clearly identify the critical intensity so that in the quantities of mean, variance, entropy and free energy of cluster size, the slope of the functions varies around a maximum point. In fact, this maximum point is exactly the same as the critical point $y_c = 1$. In part (f) of Figure 3, the zero-field free energy is plotted against the intensity parameter for the RCM. It is noticed that the zero-field free energy approaches to zero at high intensity parameter while it is $1/2$ at the critical point. Finally, we shows the kurtosis versus the intensity parameter for this model in part (c) of Figure 3. The kurtosis in statistical physics is defined by $B = \frac{\langle s_4 \rangle}{\langle s_2 \rangle^2}$, where $\langle s_2 \rangle$ and $\langle s_4 \rangle$ denote the second and fourth moments of the cluster size. Due to the sensitivity of kurtosis, these changes significantly as the intensity parameter varies. Here, the minimum value of the kurtosis coefficient occurs at the critical point. Therefore, the kurtosis, the entropy and other thermodynamic quantities can be used to determine the critical intensity value accurately.

Now, we want to know that if we use the escort probability function, these thermodynamic quantities will determine the value of the critical parameter. Using

the escort distribution in (3.10), the q -moment values is computed as

$$\chi_q^{(1)}(y) = \sum_{k=1}^{\infty} k P_{q,k}(y), \quad (3.11)$$

$$V_q(y) = \chi_q^{(2)}(\rho) - \chi_q^{(1)}(y)^2, \quad (3.12)$$

and,

$$B_q = \frac{\langle s_4 \rangle}{V_q(y)^2} \quad (3.13)$$

where,

$$\langle s_4 \rangle = \sum_{k=1}^{\infty} (k - \chi_q^{(1)}(y))^4 P_{q,k}(y)$$

The changes of the q -mean cluster $\chi_q^{(1)}(y)$ in terms of different values of y and q are shown in Figure 4. In Part (a) of this Figure, you see the $\chi_q^{(1)}(y)$ versus the size q . For $y = 1$, the curve is placed in front with a continuous line, and for values greater or less than this critical point, the curves are placed behind this curve. In the event that, by plotting the q -mean cluster against the values of intensity y and for different values of q , we see the same trend observed in Figure 3, part (a). That is, the maximum point occurs at the critical point $y_c = 1$ for different values of q . The similar changes are observed in other statistical quantities, i.e., the q -variance and the q -kurtosis, which are shown in the second and third rows of Figure 4, respectively. Here, we examine other thermodynamic quantities involving the entropy, free energy, and zero-field free energy. Using the escort distribution (3.10), the entropy and the free energy have the following non-extensive relationships.

$$S_q = - \sum_{k=1}^{\infty} P_{q,k}(y) \log P_{q,k}(y), \quad (3.14)$$

$$F_q = \sum_{k=1}^{\infty} P_{q,k}(y) \left(k + \log P_{q,k}(y) \right), \quad (3.15)$$

and, the q -zero-field free energy $F_q(y, 0)$ given as

$$\begin{aligned} F_q(y, 0) &= \sum_{k=1}^{\infty} \frac{1}{k} P_{q,k}(y) \\ &= \chi_q^{(-1)}(\rho) \end{aligned} \quad (3.16)$$

The diagram of these three non-extensive functions is shown in Figure 5. In three diagrams (a), (c) and (e), the q -entropy, q -free energy and q -zero-field free energy versus q are plotted according to different parameters, y . As can be seen in these Figures, the graph in terms of the critical point, $y_c = 1$ which denoted by a continuous line, is in front of the other graphs. In other words, the graphs drawn for $y < 1$ and $y > 1$ do not exceed this graph in the case $y_c = 1$. In parts of (b), (d) and (f) of Figure 5, the variations of these three functions are plotted against the intensity parameter for different values of q . In the q -entropy and the q -free energy, for different values of q , the maximum occurs at the critical point,

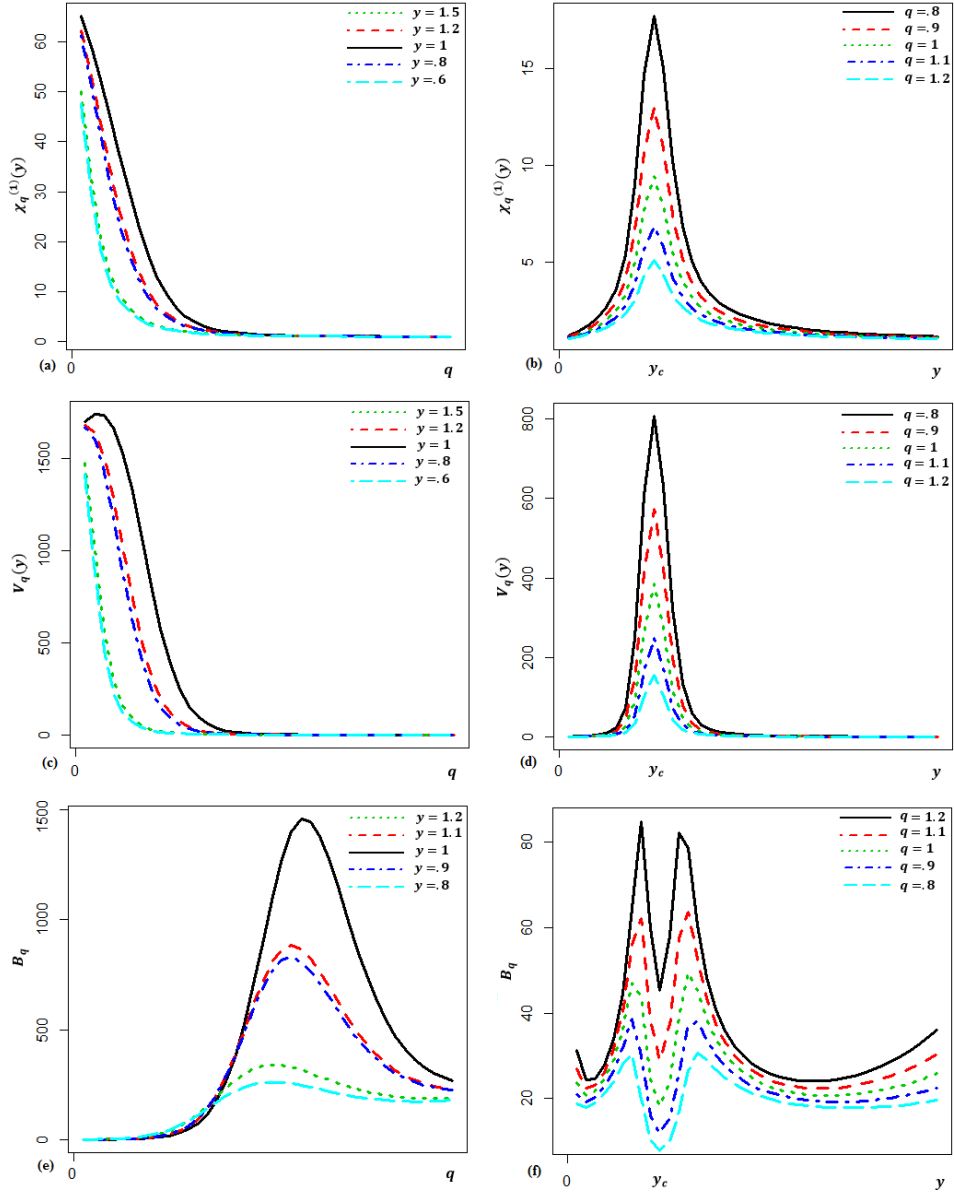


FIGURE 4. The illustration of the q -mean cluster, $\chi_q^{(1)}(y)$ (parts of a and b), the q -variance, $V_q(y)$ (parts of c and d) and the q -kurtosis, B_q (parts of e and f) in terms of the different values y and q .

while in the q -zero-field free energy, the minimum value of this function results for

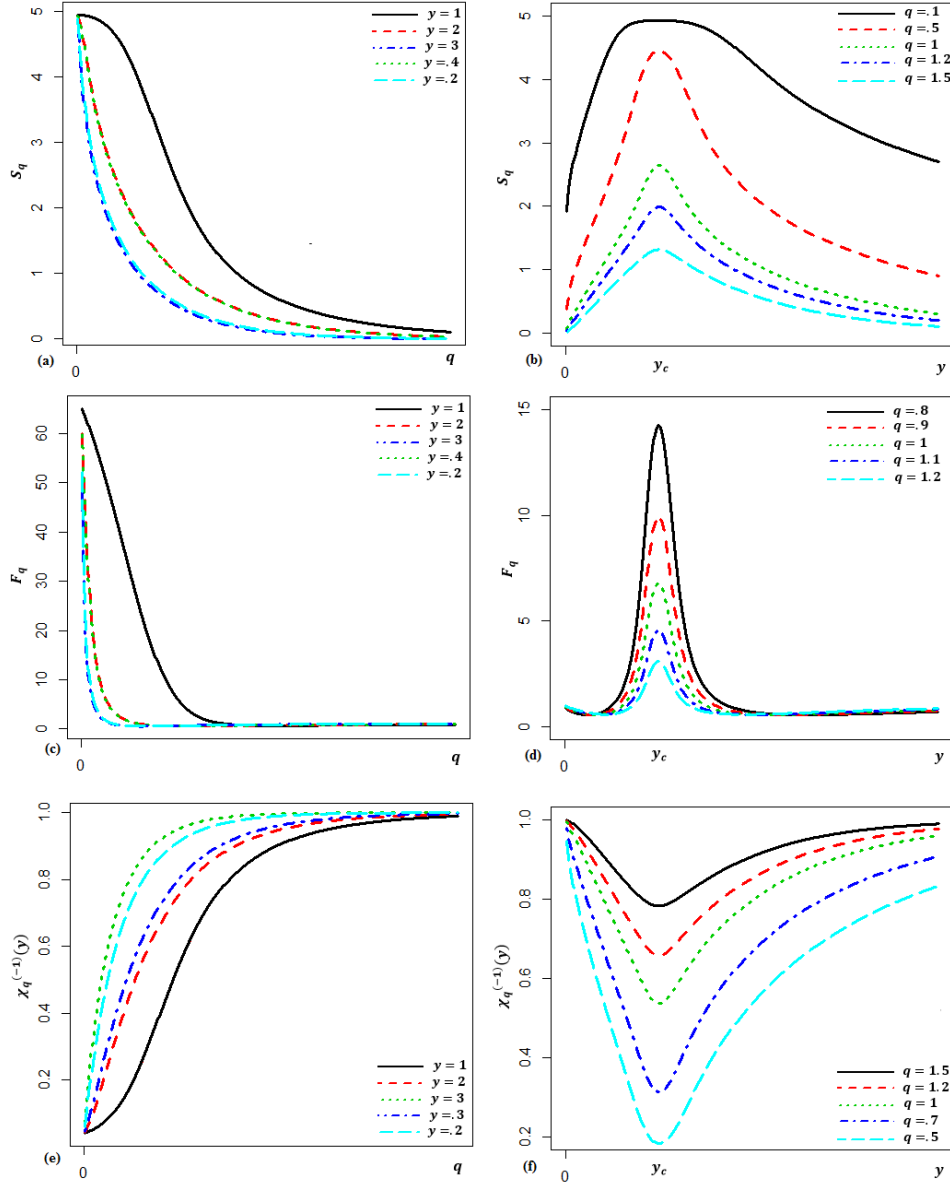


FIGURE 5. The illustration of the q -entropy, S_q (parts of *a* and *b*), the q -free energy, F_q (parts of *c* and *d*) and the q -zero-field free energy, $\chi_q^{(-1)}(y)$ (parts of *e* and *f*) in terms of the different values y and q .

any change of q at the critical point. Therefore, the q -thermodynamic quantities,

like the thermodynamic quantities, clearly show the phase transition at the critical point $y_c = 1$. The phase transition here that leads to the percolation phenomenon is in fact the formation of an infinite cluster.

4. Conclusion

We have studied the geometry associated with the escort distribution in non-extensive statistical mechanics. In the present work, we have employed the escort distribution instead of the original distribution. That is, we derived and calculated the q -expectation values and the q -moment generating function by providing some examples based on the Tsallis work. Also, using the approximation function provided by Penrose in the random connection model, the phase transition in critical point is represented by Figures from some calculated q -thermodynamic quantities. The results clearly show that the use of the escort distribution is as good as the use of the original distribution in displaying the critical point of the phase transition.

References

1. Abe, S.: Geometry of escort distributions, *Phys. Rev.E* **68** (2003), no. 3, 031101.
2. Abe, S. and Bagci, G. B.: Necessity of q -expectation value in non-extensive statistical mechanics, *Phys. Rev. E* **71** (2005), no. 1, 016139.
3. Abe, S. and Okamoto, Y.: *Non-extensive Statistical Mechanics and Its Applications*, Springer-Verlag, Heidelberg, 2001.
4. Aizenman, M., Kesten, H., and Newman, C. M.: Uniqueness of the infinite cluster and continuity of connectivity functions for short and long range percolation, *Commun. Math. Phys.* **111** (1987), no. 4, 505–531.
5. Amin, M.: Energy: The smart grid solution, *Nature* **499** (2013), no. 7457, 145–147.
6. Beck, C. and Schlögl, F.: *Thermodynamics of Chaotic Systems: An Introduction*, Cambridge University Press, Cambridge, 1993.
7. Cristina, G. A. L., Eduardo, M., Luis, F. L., and Marcos, A.: Analogy between the formulation of Ising–Glauber model and Si epidemiological model, *Appl. Math. and Phy.* **7** (2019), no. 5, 1052–1066.
8. Dawson, D. A., Gorostiza, L. G.: Percolation in a hierarchical random graph, *Communications on Stochastic Analysis* **1** (2007), no. 1, 29–47.
9. Dettmann, C. P. and Georgiou, O.: Random geometric graphs with general connection functions, *Phys. Rev. E* **93** (2016), no. 3, 032313.
10. Durrett, R. and Nguyen, B.: Thermodynamic inequalities for percolation, *Commun. Math. Phys.* **99** (1985), no. 2, 253–269.
11. Franceschetti, M. and Meester, R.: *Random networks for communication*, Cambridge University Press, 2007.
12. Gilbert, E. N.: Random plane networks, *J. Soc. Ind. Appl. Math.* **9** (1961), no. 4, 533–543.
13. Grimmett, G. R.: On the differentiability of the number of clusters per vertex in percolation model, *J. Lond. Math. Soc.* **2** (1981), no. 23, 372–384.
14. Grimmett, G. R.: *Percolation*, Springer-Verlag, New York, 1989.
15. Gunnar, J.: *Advanced Physical Chemistry: Statistical Thermodynamics*, Swiss Federal Institute of Technology Zurich, 2015.
16. Jiang, J., Zhang, S., and Guo, T.: Russo’s formula, uniqueness of the infinite cluster, and continuous differentiability of free energy for continuum percolation, *J. Appl. Prob.* **48** (2011), no. 3, 597–610.
17. Kazemi, O. K., Pourdardvish, A., and Sadeghi, J.: Phase transition in a stochastic geometry model with applications to statistical mechanics, *Math. Meth. Appl. Sci.* **8385** (2022), doi:10.1002/mma.8385.
18. Knight, K.: *Mathematical Statistics*, Chapman and Hall, CRC, 2000.
19. Levine, I. N.: *Physical Chemistry*, McGraw-Hill: University of Brooklyn, 1978.

20. Liangrong, P., Hong, Q., and Liu, H.: Thermodynamics of markov processes with nonextensive entropy and free energy, *Phys. Rev. E* **101** (2020), no. 2, 022114.
21. Mayants, L.: *The Enigma of Probability and Physics*, Springer, 1984.
22. Penrose, M. D.: Connectivity of soft random geometric graphs, *Ann. Appl. Probab.* **26** (2016), no. 2, 986–1028.
23. Penrose, M. D.: *Random geometric graphs*, Oxford University Press, Oxford, 2003.
24. Penrose, M. D.: On a continuum percolation model, *Adv. Appl. Probab.* **23** (1991), no. 3, 536–556.
25. Penrose, M. D.: Continuum percolation and euclidean minimal spanning trees in high dimensions, *Ann. Appl. Probab.* **6** (1996), no. 2, 528–544.
26. Quintanilla, J. and Torquato, S.: Clustering in a continuum percolation model, *Adv. Appl. Probab.* **29** (1997), no. 2, 327–336.
27. Rothman, K., Greenland, S., and Lash, T.: *Epidemiologia moderna*, 3rd ed., Art Med, Sao Paulo, 2011.
28. Tsallis, C.: Possible generalization of Boltzmann-Gibbs statistics, *Jour. of Stat. Phys.* **52** (1988), no. 1, 479–487.
29. Tsallis, C. and Gell-Mannin, M.: *Non-extensive Entropy: Interdisciplinary Applications*, Oxford University Press, 2003.
30. Tsallis, C., Mendes, R. S., and Plastino, A. R.: The role of constraints within generalized non-extensive statistics. *Phys. A* **261** (1998), 534–554.
31. Zhang, H. I. and Choi, M. Y.: Generalized formulation of free energy and application to photosynthesis, *Phys. A* **493** (2018), no. 2, 125–134.
32. Zhang, Y.: A derivative formula for the free energy function, *J. Stat. Phys.* **146** (2011), no. 2, 466–473.

O. K. KAZEMI : DEPARTMENT OF STATISTICS, UNIVERSITY OF MAZANDARAN, BABOLSAR, IRAN
Email address: o.kazemi@stu.umz.ac.ir

A. POURDARVISH: DEPARTMENT OF STATISTICS, UNIVERSITY OF MAZANDARAN, BABOLSAR, IRAN
Email address: a.pourdarvish@umz.ac.ir

J. SADEGHI: DEPARTMENT OF PHYSICS, UNIVERSITY OF MAZANDARAN, BABOLSAR, IRAN
Email address: pouriya@ipm.ir